Shedding Light on Axial Stress Effect on Resonance Frequencies of Nanocantilevers

Valerio Pini,[†] Javier Tamayo,[†,*] Eduardo Gil-Santos,[†] Daniel Ramos,[†] Priscila Kosaka,[†] Hien-Duy Tong,[‡] Cees van Rijn,[‡] and Montserrat Calleja[†]

[†]Instituto de Microelectrónica de Madrid, CSIC, Isaac Newton 8 (PTM), Tres Cantos, 28760 Madrid, Spain and [‡]Nanosens, Berkelkade 11, NL 7201 JE Zutphen, The Netherlands

ABSTRACT The detection back-action phenomenon has received little attention in physical, chemical, and biological sensors based on nanomechanical systems. We show that this effect is very significant in ultrathin bimetallic cantilevers, in which the laser beam that probes the picometer scale vibration largely modifies the resonant frequencies of the system. The light back-action effect is nonlinear, and some resonant frequencies can even be reduced to a half with laser power intensities of 2 mW. We demonstrate that this effect arises from the stress and strain generated by the laser heating. The experiments are explained by two-dimensional nonlinear elasticity theory and supported by finite element simulations. The found phenomenology is intimately connected to the old unsolved problem about the effect of surface stress on the resonance frequency of singly clamped beams. The results indicate that to achieve the ultimate detection limits with nanomechanical resonators one must consider the uncertainty due to the detection back-action.

KEYWORDS: cantilevers · nanomechanical sensors · optomechanics · surface stress

Light mechanical structures that oscillate at high frequencies with a very pure tone have become the basis of a variety of fascinating applications that include signal processing,[1−3] force sensing,[4,5] biological and chemical sensing,[6−16] and observation of quantum effects in mechanical systems.[3,17] These structures that are referred to as nanomechanical resonators can be shaped as cantilevers, bridges, and membranes and can even integrate micro- and nanofluidic channels.[8] A key element in these applications is the displacement transduction technique that translates the vibration of the nanomechanical resonator into a measurable electrical signal. The attainment of the last performance of these applications requires ultrahigh displacement sensitivity down to the atom size and the minimization of the "observer effect"; that is, the physical "probe" used for measuring the resonator displacement negligibly alters the mechanical state of the resonator, in this case, the resonant frequencies.

Optical techniques such as interferometry[12,18] and the laser beam deflection method[19,20] are widely used for measuring nanomechanical displacements. These techniques exhibit the advantages that they do not require electrical connections, possess the highest resolution (in the 10−100 fm/Hz$^{1/2}$ range), and can be implemented for measurements of the resonators in vacuum, gas, and liquids. In addition, it has been found that the laser beam has a negligible influence on the resonant frequencies of relatively large nanomechanical resonators such as microcantilevers with volumes on the order of 1000 μm^3 (*e.g.*, 100 μm long, 10 μm wide, and 1 μm thick).[21] However, this may not be true in the case of nanocantilevers, in which the volumes lie in the 1−10 μm^3 range.[22] The use of smaller mechanical structures is crucial for ultrasensitive mass sensing,[6,7,9,11] stiffness spectrometry,[12] and ultrasensitive force detectors,[4] to name a few applications, because of the small active masses and high resonance frequencies. In particular, the eigenfrequencies of cantilevers with nanometer-scale thickness can be influenced by the optical pressure and photothermal force generated by the laser beam probe.[22−24] The elucidation of this issue is fundamental for the development of applications based on nanomechanical resonators. Thus, the extraordinary fundamental detection limits promised by these tiny structures can be significantly impaired if the light significantly modifies the resonant frequencies. Conversely, this detriment can turn into a relevant advantage in applications consisting of active signal filtering,[2,5,25] parametric amplification,[26] and postfabrication tuning of the mechanical properties.[27−30]

In this article, we demonstrate that the laser beam used for probing the mechanical state of nanomechanical resonators can

* Address correspondence to jtamayo@imm.cnm.csic.es.

Received for review February 15, 2011 and accepted May 9, 2011.

Published online May 09, 2011
10.1021/nn200623c

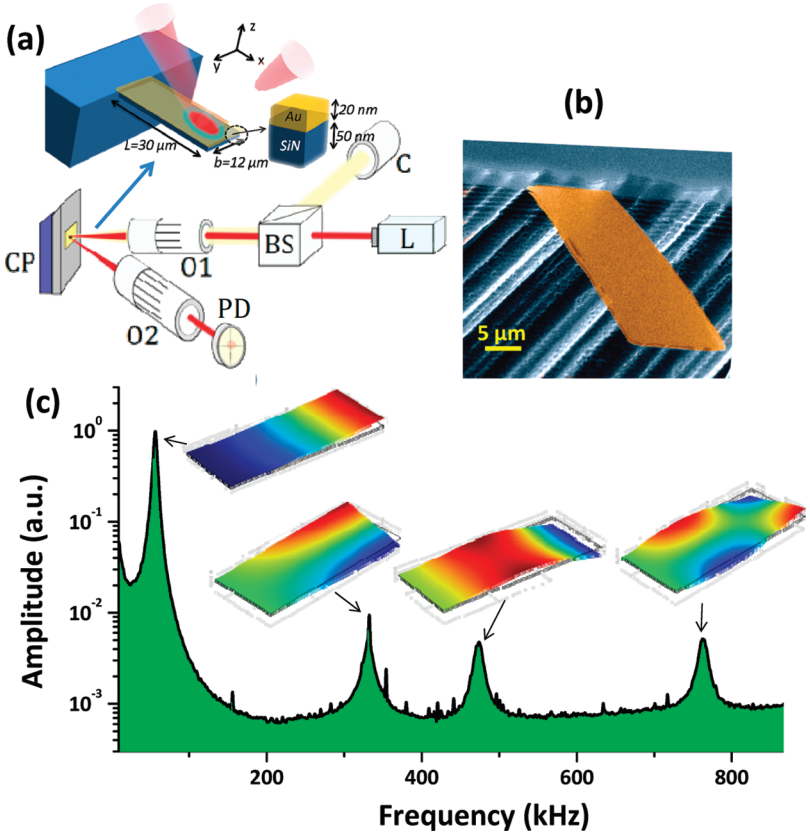

Figure 1. (a) Schematic depiction of the structure and dimensions of the fabricated bimetallic cantilever and of the laser beam deflection technique used to measure the cantilever deflection. The following component labels are used: L, laser; BS, beamsplitters; CP, Peltier cell; O1-2, microscope objective; PD, photodetector; C, camera. The path of the laser (L) is shown in red, while that of the camera light (C) is shown in yellow. In the top inset, a schematic drawing of the bimetallic cantilever used for the experiments is plotted. (b) Scanning electron microscopy of one of the fabricated cantilevers. (c) Frequency spectrum of the thermomechanical fluctuations of a cantilever. Beside each resonance peak is shown a depiction of the vibration mode shape calculated by finite element simulations.

extraordinarily shift the resonant frequencies of bimetallic ultrathin cantilevers. Strikingly, the eigenfrequency shift due to the laser back-action follows a nonlinear behavior, which reveals a new mechanism of resonance frequency shift due to in-plane stress.

RESULTS AND DISCUSSION

Here, we have fabricated arrays of bimetallic cantilevers consisting of a 50 nm thick low-stress silicon-rich silicon nitride (SiN) and 20 nm thick gold layers. The cantilevers were 30 μm long and 12 μm wide. The Au layer enhances the reflectivity of the cantilevers, and it can be easily functionalized by using self-assembly chemistry for sensing applications. A schematic of the cantilever structure and the optical detection is shown in Figure 1a. A scanning electron microscopy image of a cantilever is shown in Figure 1b. To measure the vibration properties of the cantilevers, we used a homemade laser beam deflection setup (Figure 1a).[19] The measurements were carried out in air, and the temperature of the cantilevers was controlled by means of a Peltier cell beneath the cantilever chip and a thermocouple temperature placed near the cantilever chip. The results are based on experiments carried out with eight cantilevers from three different chips.

A typical frequency spectrum of the thermomechanical noise of the fabricated cantilevers is shown in Figure 1c. The spectrum reveals the first four resonant frequencies. Simulations based on the finite element method (FEM) show a good agreement between the experimental and theoretical resonant frequencies. The FEM calculations show that the first and third resonant frequencies correspond with the first and second flexural vibration modes, whereas the second and fourth correspond with the first and second torsional vibration modes.

Let us now focus our attention on the fourth vibration mode that is the most sensitive to the light power. Figure 2a shows how its frequency largely shifts to lower frequencies when the power of the laser used to probe the mechanical state of the cantilever is increased from 1.2 to 1.4 mW for a constant temperature of about 17 °C. The laser power increase gives rise to a decrease of the resonant frequency of about 30%. To get insight into the origin of the laser-induced frequency shift, we measured the resonant frequency of

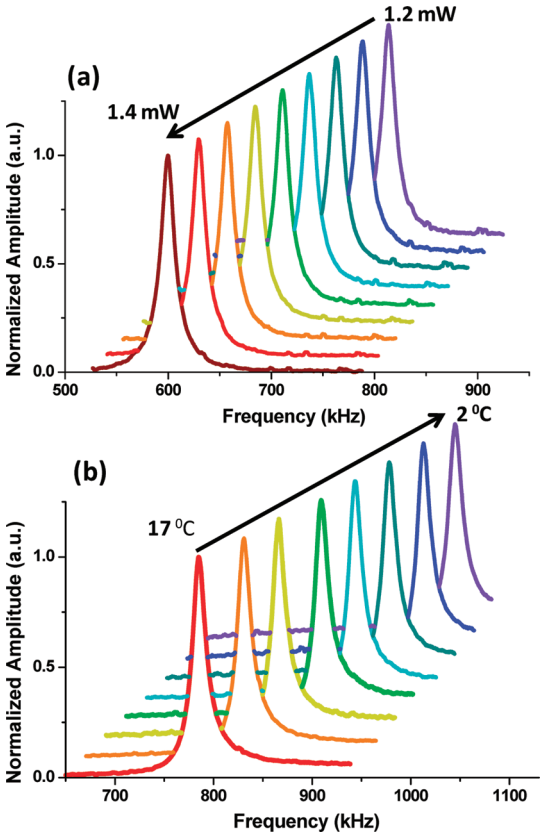

Figure 2. Evolution of the resonance peak of the fourth vibration mode as the laser power intensity used to measure the cantilever displacement is increased from 1.2 to 1.4 mW in even steps at a temperature of approximately 17 °C (a), and as the temperature is decreased from 17 to 2 °C in even steps at a laser power intensity of 1.2 mW (b). The laser beam is focused near the cantilever base.

the fourth vibration mode for a laser power of 1.2 mW as a function of the temperature (Figure 2b). The resonant frequency increased about 35% by decreasing the temperature from 17 to 2 °C. The results suggest that the laser cantilever heating is the mechanism responsible for the downward frequency shift. The absorbed power depends on the optical frequency of the excitation laser, the imaginary part of the refraction index of the cantilever layers, and the angle between the incident beam and the cantilever.[23] In our conditions, we estimate a theoretical light power absorption of about 13%. By applying the heat diffusion equation to a Gaussian heating source to mimic the experimental laser spot, we calculate the distribution of temperature across the cantilever induced by 1 mW incident laser beam (Figure 3). When the laser beam is focused near the free cantilever end, the temperature quickly decays toward the support, whereas it approximately remains constant toward the tip. This arises from the low heat transfer by air convection that forces the heat to flow toward the chip. Thus, when the laser is focused near the clamping region, the induced temperature increase is uniform along the cantilever except near the base. Since the optical displacement sensing technique is sensitive to discern the resonant frequencies from the thermomechanical noise even for the laser beam incident near the base, hereinafter, we will discuss the case in which the laser is focused near the cantilever base. In this case, in order to simplify the theoretical model, we can consider the temperature distribution across the cantilever to be approximately constant and on the order of 0.01 K/μW, which is consistent with our experimental results. As discussed below, this assumption allows us to connect this phenomenon with the controversial problem of the effect of surface stress on the cantilever eigenfrequencies.

Figure 4a shows the first four resonant frequencies of a microcantilever plate as a function of the laser power. In Figure 4b, the relative frequency shifts are plotted. The uncertainty in both the laser spot position on the cantilever and spot size gives rise to an error in the frequency of 0.2% that is smaller than the symbol size in Figure 4. Interestingly, the resonant frequency shifts follow a nonlinear behavior with the laser power. In addition, the relative frequency shift depends on the vibration mode index and on the kind of motion. The torsional modes, second and fourth vibration modes, are more sensitive to the laser power than the flexural modes (first and third mode). In this nanomechanical system, the second torsional mode is the mode that shows more laser back-action effect. Its frequency is reduced 40 $\pm$ 10% by illuminating the cantilever with a power intensity of 2 mW, reaching a state in which the third and fourth eigenmodes are close to being degenerated in frequency. Thus, this extraordinary light-tuning of the eigenfrequencies can lead to "exotic" situations in the dynamic response of these nanomechanical resonators such as the alteration in the frequency order of the vibration modes.

Most of the methods to tune the resonance frequency of nanomechanical resonators are based on controlling the stress of the beam by mechanical,[30] electrical,[29] and thermal effects.[27,31] Here we use the light to control the stress of the beam. However, the most relevant difference is that the applicability of the aforementioned methods is limited to constrained structures such as doubly clamped beams where the stress cannot relax by expanding or contracting. In our case, the mechanical structure is an ultrathin microcantilever plate, and since the cantilever free end is unrestrained, most of the axial force along the beam can be relieved through the beam deformation.[32,33] Well-established mechanisms that can modify the resonance frequencies of singly clamped beams are the temperature dependence of the Young's modulus and the thermal elongation of the cantilever.[34] Both mechanisms induce a linear change of the resonant frequencies below 10^{-5} K^{-1} that is between 1 and 2 orders of magnitude lower than the values found here. In addition, the frequency shifts follow a nonlinear

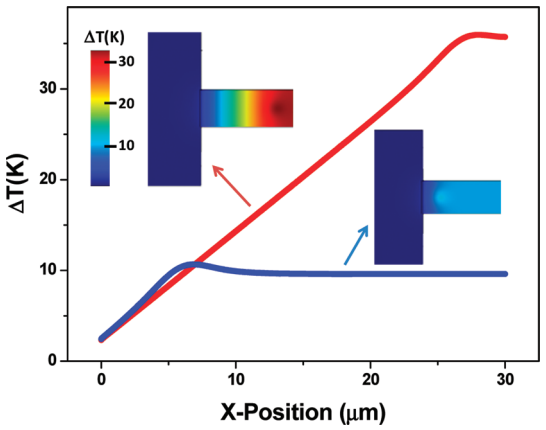

Figure 3. Cross sections along the cantilever of the simulated laser-induced heating for a Gaussian spot at 6 μm from the base (blue line) and at 3 μm from the cantilever tip (red line). The *x*-axis origin is the clamped cantilever end. The laser power is 1 mW, and the beam waist is 3 μm. The two-dimensional intensity color maps of the temperature increase across the cantilever and chip are also shown.

behavior. To unveil the mechanism responsible for the frequency tuning in singly clamped beams, we model the effect of a uniform temperature change, induced by the laser beam, on a bimetallic rectangular cantilever by using large deformation two-dimensional elasticity. It is interesting to emphasize that the phenomenology found here is qualitatively the same if the change of temperature was substituted by a change of strain-independent surface stress on the opposite surfaces of the cantilever. This is a classical problem in mechanics that has been largely studied during the last three decades, in which a consensus on the solution has not been achieved yet.[32,33]

The problem can be simplified to a two-dimensional isotropic beam subject to a biaxial bending moment per width unit (M_{th}) due to the difference in thermal expansion of the SiN and Au layers and a biaxial in-plane force per width unit (N_{th}) due to the thermal expansion of the beam given by[35]

$$M_{th} \cong \frac{E_f h_f h_s}{2(1-\upsilon_f^2)}[\alpha_f(1+\upsilon_f) - \alpha_s(1+\upsilon_s)]\Delta T \quad (1)$$

$$N_{th} \cong \left(\frac{E_s \alpha_s h_s}{1-\upsilon_s} + \frac{E_f \alpha_f h_f}{1-\upsilon_f}\right)\Delta T \quad (2)$$

where E is the Young's modulus, υ is the Poisson's ratio, α is the thermal expansion coefficient, ΔT is the temperature variation, h is the layer thickness, and the subscripts s and f denote the substrate (SiN) and the deposited film (Au), respectively. The bending moment, M_{th}, causes the cantilever to bend with a curvature radius, κ, that is approximately given by $\kappa = M_{th}/D$, where D is the flexural rigidity of the beam. So far, the influence of M_{th} on the resonance frequency of cantilevers has been neglected, pointing out the biaxial stress, N_{th}, as the main suspect in the resonance frequency shifts. The reasoning is based on simplifying

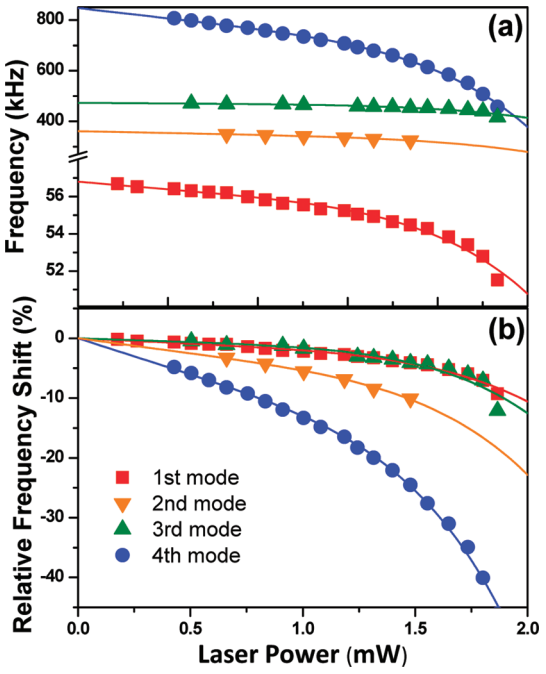

Figure 4. First four resonant frequencies of a microcantilever plate as a function of the laser power intensity; (a) the frequency values are shown, and (b) the relative frequency shifts are calculated with respect to the extrapolated frequency value at zero laser power intensity.

the cantilever as a taut string whose frequency largely depends on the string tension. However, as mentioned above, this approach is not physically justified as the free cantilever end is unrestrained[33] and most of the in-plane stress relaxes except in a small region near the clamp that induces a moderate change of the fundamental resonance frequency.[32] In our case, this effect should induce an eigenfrequency increase of about 0.03% per Kelvin. This shift is of opposite sign to our experimental results and between 1 and 2 orders of magnitude smaller than the experimental values.

The finite element simulations show no effect of the temperature on the eigenfrequencies when a linear relation between strain and displacements is assumed. However, a significant effect is obtained by applying nonlinear von Karman's strain/displacement relations:[36]

$$\varepsilon_{ij} = \frac{1}{2}\left(\frac{\partial u_i}{\partial x_j} + \frac{\partial u_j}{\partial x_i} + \frac{\partial u_k}{\partial x_i}\frac{\partial u_k}{\partial x_j}\right) \quad (3)$$

where ε_{ij} is the Lagrangian finite strain tensor ($i,j = 1, 2, 3$), u_i is the displacement vector, and x_i is the Cartesian coordinates. Figure 5a shows the simulation results of the eigenfrequency shifts *versus* the temperature variation. Except for the first vibration mode when the temperature increases below 5 K, the resonant frequencies decrease for positive and negative variations of the temperature. Notice that the zero-temperature variation corresponds in our simulations to the cantilever without thermal strain (*i.e.*, null deflection).

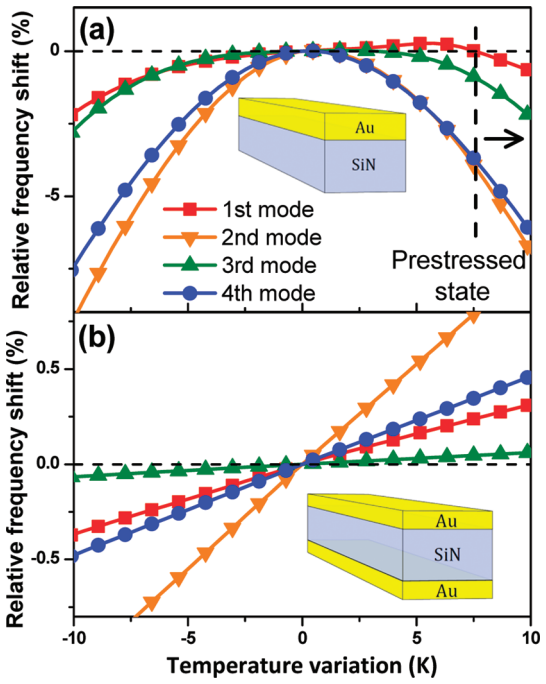

Figure 5. (a) Finite element simulations of the relative shift of the first four eigenfrequencies as a function of the cantilever temperature. In these simulations, the zero temperature corresponds with the cantilever without thermal strain. The simulated cantilever consists of a bilayer of 20 nm of Au and 50 nm of silicon nitride (inset). The vertical dashed line approximately indicates the value of initial stress measured in the fabricated devices at room temperature. (b) Finite element simulations of the relative shift of the first four eigenfrequencies as a function of the cantilever temperature for a cantilever consisting of a trilayer of 10 nm of Au, 50 nm of silicon nitride, and 10 nm of Au (inset).

Experimentally, the cantilever is in a prestressed state at room temperature as a consequence of the fabrication residual stress. White light interferometry experiments show that the cantilevers are initially bent downward (toward the SiN) about 1 μm at room temperature with a bending responsivity to the temperature of about 60 nm/K. The found residual deflection is obtained in our simulations at $\Delta T = 8$ K (vertical dashed line in Figure 5a). The theoretical eigenfrequency shifts for temperatures above this value are similar to those found experimentally. Consistent with the experiments, the torsional modes are more sensitive to the temperature. It is important to emphasize that the presented phenomenon is strongly nonlinear, and the initial residual stress then determines the dependence of the eigenfrequencies on the temperature and surface stress. For instance, if the cantilever would be initially bent upward (toward the Au), the eigenfrequency shifts would be positive with the temperature. The main discrepancy between the theory and the experiments is found for the first torsional mode (second eigenfrequency) that shows, in the simulation, a temperature sensitivity similar to the second torsional mode (fourth eigenmode), whereas in the experiments, this sensitivity is significantly smaller (Figure 4b). These discrepancies are reasonable as the heating induced by the laser beam is not uniform near the base (Figure 3).

As described above, the temperature induces a bending moment (eq 1) and an unreleased axial stress near the clamp (eq 2). To decouple both effects, we simulate the effect of the temperature on a cantilever in which half of the gold layer is adhered to the bottom surface and the other half to the top (Figure 5b). In this symmetric trilayer structure, the temperature does not induce a cantilever bending, and the only effect that can shift the eigenfrequencies is the unreleased axial stress. The simulations show that the resonant frequencies linearly depend on the temperature. The absolute frequency shifts are about 1 order of magnitude smaller than in the bimetallic cantilever. The data for the first flexural mode are similar to those obtained by applying the previous model of unrelieved surface stress effect on the resonance frequency.[32] The simulations indicate that the effects of the bending moment and unrelieved axial stress on the resonance frequencies can be distinguished by their temperature dependence: the axial stress effect is odd, whereas the cantilever bending effect is even. Our results indicate that the previous model of strain-independent surface stress effect is valid for cantilevers with low residual stress and small deflection induced by the surface stress.[32] However, it fails to explain the effects when either large surface stress (residual and adsorption-induced) occurs or ultrathin cantilevers are used. In fact, surface stress mechanics usually assumes that cantilever displacements are small with regard to the cantilever thickness. However, this assumption is extremely restrictive from the experimental point of view where large deflections are sought for small surface stress variations. This restriction is particularly critical not only for ultrathin microcantilevers but also for nanowires and nanotubes that are able to deflect orders of magnitude of their thicknesses with very small stresses/forces.

CONCLUSION

In conclusion, nanomechanical resonators increasingly smaller are pursued to achieve unprecedented detection limits in mass sensing, stiffness spectrometry, and force measurements. The mechanical state, that is, displacement and vibration, can be sensitively measured by optical techniques. Here we show that the optical beam significantly alters the eigenfrequencies of the singly clamped nanobeams. The same phenomenon is expected for the static deformation, although it has not been examined here. The measurement back-action imposes a limit in the accuracy of the measurement, and it may prevent the achievement of the fundamental

detection limits established so far.[1] This coupling is also expected for electrical detection techniques that inherently generate Joule heating. Therefore, when ultrathin cantilever, nanowires, or nanotubes are used, methods must be developed to reconstruct the unperturbed mechanical state in order to achieve a highly sensitive and reliable measurement. Moreover, the results shed light on the effect of surface stress on nanomechanical sensors. Surface stress (or bimetallic) effect on cantilevers has two components: (i) the unreleased axial stress and (ii) the deflection induced by the bending moment. The second effect, which has been traditionally ignored, has been revealed as the most important contribution in the case of ultrathin cantilevers. These two effects can be distinguished by studying their functional parity; the axial stress effect is odd, whereas the bending moment effect is even.

EXPERIMENTAL METHODS

Cantilever Fabrication. A 4 in. 380 μm thick, double side polished ⟨100⟩ Si wafer was coated with 300 nm of wet-thermal silicon dioxide (SiO_2) and 50 nm of low-stress silicon-rich silicon nitride (SiN) by means of low-pressure chemical vapor deposition (LPCVD). A first microlithography procedure was then carried out to define the cantilever patterns on a photoresist layer on the front-side of the wafer, followed by a dry ($CHF_3 + O_2$) etching of the SiN to etch the exposed silicon nitride film. This etching step was controlled to stop on the SiO_2 film. Afterward, the photoresist was stripped in an oxygen plasma. Subsequently, the second microlithography procedure, followed by e-beam metal evaporation, and standard lift-off technique were carried out to pattern the Au areas on the cantilevers. The evaporated Au film had a thickness of 20 nm with an adhesion layer of 5 nm thick chromium. Then, windows were aligned and created on the back-side of the wafer by the third microlithography procedure, followed by a through-wafer dry etching step (using a Bosch process with a SF_6/O_2 gas mixture). This through-wafer etching is controlled to stop when a sacrificial film of SiO_2 is reached. The front-side (Au and nitride films) was protected during the dry etching procedure by a photoresist layer. Next, the photoresist film was stripped in an oxygen plasma oven, followed by wet etching of the SiO_2 layer in a diluted buffered oxide etch solution to reveal the free-standing SiN/Au bimetallic cantilevers. It should be noted that the cantilever wafer was transferred directly from the wet-etch solution into a beaker containing distilled water and several surfactants to reduce surface tension. This procedure drastically improves the fabrication yield from about 50% (without this step) up to 90%. Finally, the wafer was manually separated into single chips with dimensions of 3 mm × 1.7 mm containing four cantilever beams.

Optical Setup. To measure the vibration properties of the cantilevers, we used a homemade laser beam deflection setup[19] (Figure 1a). The measurements were carried out in air, and the temperature of the cantilevers was controlled by means of a Peltier cell beneath the cantilever chip and a thermocouple temperature placed near the cantilever chip. The beam from an intensity-modulated laser diode (λ = 780 nm) was directed to the sample through a 20× objective with a numerical aperture of 0.42. The spot size was 2−3 μm. The light reflected off the cantilevers was collected by a second objective (10×, NA = 0.28) and then by a quadrant photodetector. The segment photocurrents were amplified by low-noise current to voltage preamplifiers and acquired by a high-speed voltage digitizer connected to a PC.

Finite Element Simulations. Finite element simulations were performed with commercial software Comsol 4.0. The simulation process consists of two sequential steps. First, we calculated the static cantilever displacement when the cantilever is subject to a temperature change uniformly distributed. This study includes the calculation of large deformation effects that arise from the geometric nonlinearity. In this case, the Green strain tensor and the second Piola−Kirchhoff stress tensors are used and the solution is achieved by using a total Lagrangian formulation. In the second part of the simulation, we obtain the cantilever eigenfrequencies by including the static cantilever deformation calculated previously. In order to avoid long-time-consuming simulations and to obtain accurate solutions, the meshing of the cantilever structure that has large aspect ratio must be individually adapted to each direction. We applied a customized free tetrahedral meshing. In addition, since the stress and strain near the clamping region play a critical role in the vibration response of the cantilevers, the clamping region was refined with an extremely fine meshing. A convergence study was performed by refining the mesh element size until the relative error in the cantilever eigenfrequency was below 10^{-4}. This corresponds to a mesh of 500 000 elements, approximately.

Acknowledgment. The authors acknowledge financial support from the Spanish Science Ministry through Projects TEC2009-14517-C02, TRA2009-0117, and CSD2007-00010. We thank Alberto Cagliani for his assistance in the finite element simulations.

REFERENCES AND NOTES

1. Ekinci, K.; Roukes, M. Nanoelectromechanical Systems. *Rev. Sci. Instrum.* **2005**, *76*, 061101.
2. Erbe, A.; Krommer, H.; Kraus, A.; Blick, R.; Corso, G.; Richter, K. Mechanical Mixing in Nonlinear Nanomechanical Resonators. *Appl. Phys. Lett.* **2009**, *77*, 3102–3104.
3. Steele, G.; Huttel, A.; Witkamp, B.; Poot, M.; Meerwaldt, H.; Kouwenhoven, L.; van der Zant, H. Strong Coupling between Single-Electron Tunneling and Nanomechanical Motion. *Science* **2009**, *325*, 1103.
4. Degen, C.; Poggio, M.; Mamin, H.; Rettner, C.; Rugar, D. Nanoscale Magnetic Resonance Imaging. *Proc. Natl. Acad. Sci. U.S.A.* **2009**, *106*, 1313.
5. Li, M.; Tang, H.; Roukes, M. Ultra-sensitive NEMS-Based Cantilevers for Sensing, Scanned Probe and Very High-Frequency Applications. *Nat. Nanotechnol.* **2007**, *2*, 114–120.
6. Varshney, M.; Waggoner, P.; Tan, C.; Aubin, K.; Montagna, R.; Craighead, H. Prion Protein Detection Using Nanomechanical Resonator Arrays and Secondary Mass Labeling. *Anal. Chem.* **2008**, *80*, 2141–2148.
7. Naik, A.; Hanay, M.; Hiebert, W.; Feng, X.; Roukes, M. Towards Single-Molecule Nanomechanical Mass Spectrometry. *Nat. Nanotechnol.* **2009**, *4*, 445–450.
8. Burg, T.; Godin, M.; Knudsen, S.; Shen, W.; Carlson, G.; Foster, J.; Babcock, K.; Manalis, S. Weighing of Biomolecules, Single Cells and Single Nanoparticles in Fluid. *Nature* **2007**, *446*, 1066–1069.
9. Jensen, K.; Kim, K.; Zettl, A. An Atomic-Resolution Nanomechanical Mass Sensor. *Nat. Nanotechnol.* **2008**, *3*, 533–537.
10. Waggoner, P.; Craighead, H. Micro- and Nanomechanical Sensors for Environmental, Chemical, and Biological Detection. *Lab Chip* **2007**, *7*, 1238–1255.
11. Lassagne, B.; Garcia-Sanchez, D.; Aguasca, A.; Bachtold, A. Ultrasensitive Mass Sensing with a Nanotube Electromechanical Resonator. *Nano Lett.* **2008**, *8*, 3735–3738.
12. Gil-Santos, E.; Ramos, D.; Martínez, J.; Fernández-Regúlez, M.; García, R.; San Paulo, Á.; Calleja, M.; Tamayo, J. Nanomechanical Mass Sensing and Stiffness Spectrometry Based on Two-Dimensional Vibrations of Resonant Nanowires. *Nat. Nanotechnol.* **2010**, *5*, 641–645.

13. Dohn, S.; Svendsen, W.; Boisen, A.; Hansen, O. Mass and Position Determination of Attached Particles on Cantilever Based Mass Sensors. *Rev. Sci. Instrum.* **2007**, *78*, 103303.
14. Braun, T.; Ghatkesar, M.; Backmann, N.; Grange, W.; Boulanger, P.; Letellier, L.; Lang, H.; Bietsch, A.; Gerber, C.; Hegner, M. Quantitative Time-Resolved Measurement of Membrane Protein−Ligand Interactions Using Microcantilever Array Sensors. *Nat. Nanotechnol.* **2009**, *4*, 179–185.
15. Arcamone, J.; Sansa, M.; Verd, J.; Uranga, A.; Abadal, G.; Barniol, N.; van den Boogaart, M.; Brugger, J.; Pérez Murano, F. Nanomechanical Mass Sensor for Spatially Resolved Ultrasensitive Monitoring of Deposition Rates in Stencil Lithography. *Small* **2009**, *5*, 176–180.
16. Arlett, J.; Myers, E.; Roukes, M. Comparative Advantages of Mechanical Biosensors. *Nat. Nanotechnol.* **2011**, *6*, 203–215.
17. Naik, A.; Buu, O.; LaHaye, M.; Armour, A.; Clerk, A.; Blencowe, M.; Schwab, K. Cooling a Nanomechanical Resonator with Quantum Back-Action. *Nature* **2006**, *443*, 193–196.
18. Kouh, T.; Karabacak, D.; Kim, D.; Ekinci, K. Diffraction Effects in Optical Interferometric Displacement Detection in Nanoelectromechanical Systems. *Appl. Phys. Lett.* **2009**, *86*, 013106.
19. Ramos, D.; Arroyo-Hernández, M.; Gil-Santos, E.; Duy Tong, H.; Van Rijn, C.; Calleja, M.; Tamayo, J. Arrays of Dual Nanomechanical Resonators for Selective Biological Detection. *Anal. Chem.* **2009**, *81*, 2274–2279.
20. Kosaka, P. M. T., J.; Gil-Santos, E.; Mertens, J.; Pini, V.; Martínez, N. F.; Ahumada, O.; Calleja, M. Simultaneous Imaging of the Topography and Dynamic Properties of Nanomechanical Systems by Optical Beam Deflection Microscopy. *J. Appl. Phys.* **2011**, *109*, 064315.
21. Allegrini, M.; Ascoli, C.; Baschieri, P.; Dinelli, F.; Frediani, C.; Lio, A.; Mariani, T. Laser Thermal Effects on Atomic Force Microscope Cantilevers. *Ultramicroscopy* **1992**, *42*, 371–378.
22. Sadeghian, H.; Yang, C.; Gavan, K.; Goosen, J.; van der Drift, E.; van der Zant, H.; Bossche, A.; French, P.; van Keulen, F. Some Considerations of Effects-Induced Errors in Resonant Cantilevers with the Laser Deflection Method. *J. Micromech. Microeng.* **2010**, *20*, 105027.
23. Ramos, D.; Tamayo, J.; Mertens, J.; Calleja, M. Photothermal Excitation of Microcantilevers in Liquids. *J. Appl. Phys.* **2006**, *99*, 124904.
24. Vassalli, M.; Pini, V.; Tiribilli, B. Role of the Driving Laser Position on Atomic Force Microscopy Cantilevers Excited by Photothermal and Radiation Pressure Effects. *Appl. Phys. Lett.* **2010**, *97*, 143105.
25. Masmanidis, S.; Karabalin, R.; De Vlaminck, I.; Borghs, G.; Freeman, M.; Roukes, M. Multifunctional Nanomechanical Systems *via* Tunably Coupled Piezoelectric Actuation. *Science* **2007**, *317*, 780.
26. Rhoads, J.; Shaw, S.; Turner, K. Nonlinear Dynamics and Its Applications in Micro- and Nanoresonators. *J. Dyn. Syst., Meas., Control* **2010**, *132*, 034001.
27. Jun, S.; Huang, X.; Manolidis, M.; Zorman, C.; Mehregany, M.; Hone, J. Electrothermal Tuning of Al−SiC Nanomechanical Resonators. *Nanotechnology* **2006**, *17*, 1506.
28. Kim, K.; Jensen, K.; Zettl, A. Tuning Nanoelectromechanical Resonators with Mass Migration. *Nano Lett.* **2009**, *9*, 3209–3213.
29. Kozinsky, I.; Postma, H.; Bargatin, I.; Roukes, M. Tuning Nonlinearity, Dynamic Range, and Frequency of Nanomechanical Resonators. *Appl. Phys. Lett.* **2009**, *88*, 253101.
30. Verbridge, S.; Shapiro, D.; Craighead, H.; Parpia, J. Macroscopic Tuning of Nanomechanics: Substrate Bending for Reversible Control of Frequency and Quality Factor of Nanostring Resonators. *Nano Lett.* **2007**, *7*, 1728–1735.
31. Larsen, T.; Schmid, S.; Gronberg, L.; Niskanen, A.; Hassel, J.; Dohn, S.; Boisen, A. Ultrasensitive String-Based Temperature Sensors. *Appl. Phys. Lett.* **2011**, *98*, 121901-3.
32. Lachut, M.; Sader, J. Effect of Surface Stress on the Stiffness of Cantilever Plates. *Phys. Rev. Lett.* **2007**, *99*, 206102.
33. Lu, P.; Lee, H.; Lu, C.; O'Shea, S. Surface Stress Effects on the Resonance Properties of Cantilever Sensors. *Phys. Rev. B* **2005**, *72*, 85405.
34. Mertens, J.; Finot, E.; Thundat, T.; Fabre, A.; Nadal, M. H.; Eyraud, V.; Bourillot, E. Effects of Temperature and Pressure on Microcantilever Resonance Response. *Ultramicroscopy* **2003**, *97*, 119–126.
35. Hsueh, C. H. Modeling of Elastic Deformation of Multilayers Due to Residual Stresses and External Bending. *J. Appl. Phys.* **2002**, *91*, 9652.
36. Harper, B.; Chih-Ping, W. A Geometrically Nonlinear Model for Predicting the Intrinsic Film Stress by the Bending-Plate Method. *Int. J. Solids Struct.* **1990**, *26*, 511–525.